ACS OMEGA

http://pubs.acs.org/journal/acsodf

Article

Influence of the Underlying Substrate on the Physical Vapor Deposition of Zn-Phthalocyanine on Graphene

Timothy Mirabito, Benjamin Huet,* Joan M. Redwing, and David W. Snyder*

Cite This: *ACS Omega* 2021, 6, 20598−20610

Read Online

ACCESS | Metrics & More | Article Recommendations | Supporting Information

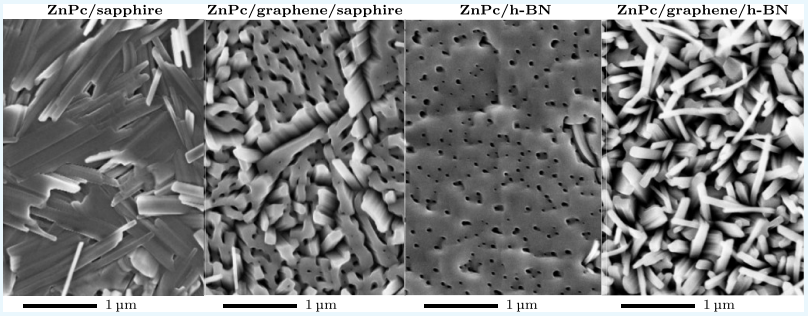

ABSTRACT: Graphene shows great promise not only as a highly conductive flexible and transparent electrode for fabricating novel device architectures but also as an ideal synthesis platform for studying fundamental growth mechanisms of various materials. In particular, directly depositing metal phthalocyanines (MPc's) on graphene is viewed as a compelling approach to improve the performance of organic photovoltaics and light-emitting diodes. In this work, we systematically investigate the ZnPc physical vapor deposition (PVD) on graphene either as-grown on Cu or as-transferred on various substrates including Si(100), C-plane sapphire, SiO_2/Si, and h-BN. To better understand the effect of the substrate on the ZnPc structure and morphology, we also compare the ZnPc growth on highly crystalline single- and multilayer graphene. The experiments show that, for identical deposition conditions, ZnPc exhibits various morphologies such as high-aspect-ratio nanowires or a continuous film when changing the substrate supporting graphene. ZnPc morphology is also found to transition from a thin film to a nanowire structure when increasing the number of graphene layers. Our observations suggest that substrate-induced changes in graphene affect the adsorption, surface diffusion, and arrangement of ZnPc molecules. This study provides clear guidelines to control MPc crystallinity, morphology, and molecular orientations which drastically influence the (opto)electronic properties.

INTRODUCTION

Organic photovoltaics (OPVs) are positioned to play a key role in the future of solar cells due to their mass producibility and low cost. Over the last two decades, metal phthalocyanines (MPc's) have been frequently utilized as the active material in these OPVs owing to their high absorption coefficient in the visible spectrum, good chemical stability, and tunable properties.[1,2] As part of the device design, the substrate interaction, molecular orientation, and overall morphology play a decisive role in determining the electronic properties.[3] Zinc phthalocyanine (ZnPc), in particular, is often used as a model for fundamental studies as it is nontoxic and easily synthesized and shares most of the physical properties of other MPc molecules.[4,5]

Significant research effort has been dedicated to understanding the MPc/substrate interface in order to produce high-quality thin films with improved electron transfer and light absorption.[6] The MPc/substrate interaction was first studied using single-crystalline metals such as Cu(111),[7−9] Au(111),[5,10,11] and Ag(111).[12,13] More recently, there has been a growing interest for integrating graphene into organic electronic devices in order to exploit its combination of flexibility, excellent conductivity, and high optical transparency.[14−16] Hence, various studies investigated the molecule−substrate interactions and the self-assembly of the MPc structure deposited on graphene epitaxially grown on SiC(0001),[17,18] Ru(0001),[19] Ni(111),[20,21] Pt(111),[22] and so forth. While these studies achieved important milestones in better understanding the interfacial coupling between MPc molecules and graphene, they mostly focused on self-assembled ultrathin (i.e., submonolayer) MPc films deposited in ultrahigh vacuum equipment.

Received: May 26, 2021
Accepted: July 15, 2021
Published: July 27, 2021

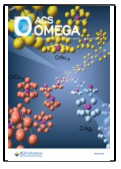

https://doi.org/10.1021/acsomega.1c02758
ACS Omega 2021, 6, 20598−20610

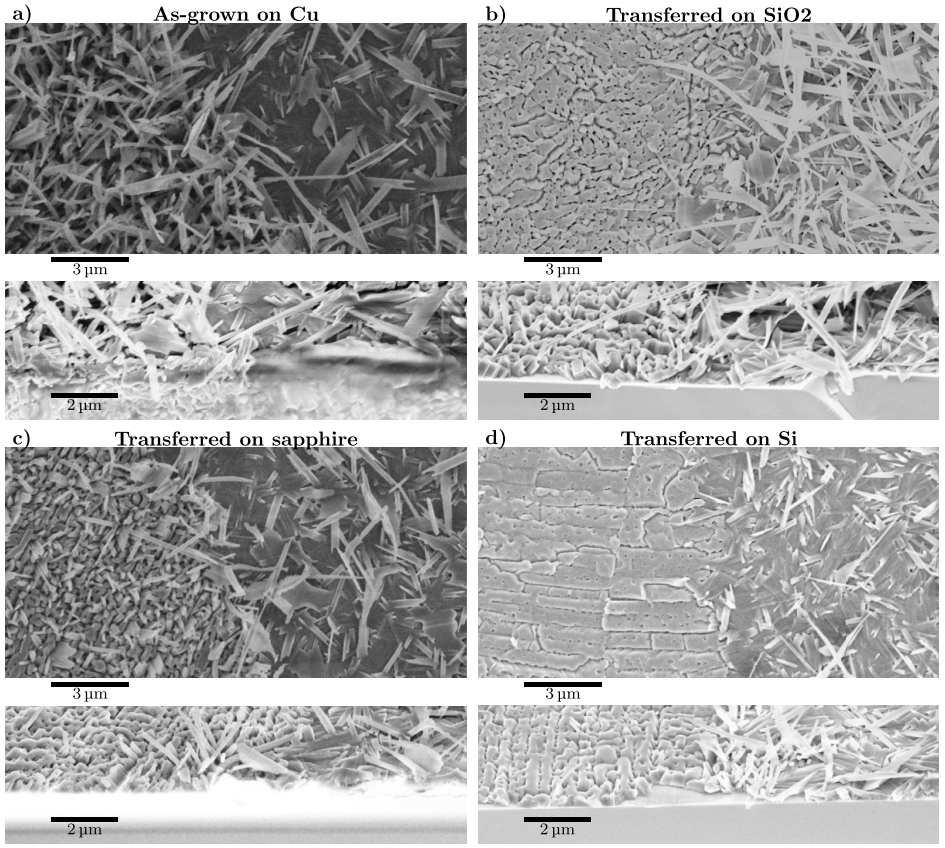

Figure 1. Plan-view (top) and side-view (bottom) SEM images (in-lens detector) of ZnPc deposited by PVD using a source temperature of 450 °C, a substrate temperature of 250 °C, and a deposition duration of 30 s. ZnPc is deposited on both graphene (left side) and on the bare substrate (right side) which is either (a) Cu, (b) SiO_2, (c) C-plane sapphire, or (d) silicon.

Until now, only a few research groups employed CVD graphene as a synthesis template for the MPc deposition. However, their research interests were primarily limited to either manipulating the molecular orientation to optimize the electronic coupling at the MPc−substrate interface[23,24] or growing vertical nanowires for photovoltaic,[25,26] sensing,[27] and biocidal[28] applications. Moreover, these studies did not exploit the ability of CVD graphene to be transferred onto a wide variety of substrates and overlooked the fact that the underlying substrate can strongly influence the behavior of molecules deposited on top of the one-atom-thick graphene layer as it has been shown for III−V compounds or other 2D materials.[29,30] Finally, none of these studies used the state-of-the-art CVD graphene with a high crystallinity and a controlled number of layers which is essential to obtain consistent and uniform deposition conditions over large areas.

Herein, we report a systematic study evaluating how the ZnPc growth is impacted by various substrate parameters including the type of substrate underneath graphene, the number of graphene layers, and graphene morphological features such as wrinkles and ripples. ZnPc growth is first achieved on single-layer CVD graphene either as-grown on Cu or as-transferred onto technologically relevant substrates such as Si(100), SiO_2/Si, and C-plane sapphire. In order to shed some light on the transparency of graphene and the role of the underlying substrate, we also investigated the ZnPc deposition on highly crystalline multilayer graphene (from 1 to 4 layers) and the use of exfoliated highly oriented pyrolytic graphene (HOPG) and hexagonal boron nitride (h-BN) as a spacer/screen/buffer between CVD graphene and the substrate. Our experimental results demonstrate that, under identical physical vapor deposition (PVD) conditions, the ZnPc film can either adopt a coalesced thin film or a high-aspect-ratio nanowire morphology depending on both the number of graphene layers and the nature of the supporting substrate. The underlying mechanisms for these observations are discussed based on electrostatic doping, strain, surface energy, polar field, surface purity/features, and structural defects. This research provides new routes to control the ZnPc film key characteristics (e.g., roughness, continuity, crystallinity, morphology, and molecular orientation) which determine charge carrier transport and interaction with light and ultimately device performance.

EXPERIMENTAL METHODS

For this study, graphene was produced by chemical vapor deposition (CVD) using 50 μm-thick Cu foils (Goodfellow, USA, Cu 99.9%). Millimeter-size single-crystalline graphene domains are obtained using in situ annealing of the Cu foil in Ar prior to graphene growth, as described in our previous study.[31] Large crystalline multilayer graphene regions were achieved by suspending the Cu foil in the CVD reactor in order to promote the adsorption of methane on both sides of the catalyst.[31] Graphene was then transferred onto various substrates using the wet PMMA-assisted transfer method reported in ref 32. The substrates include Si(100) from Addison Engineering (USA), 90 nm-thick wet oxide on Si from Addison Engineering (USA), and C-plane sapphire from Cryscore Optoelectronic (China).

https://doi.org/10.1021/acsomega.1c02758
ACS Omega 2021, 6, 20598−20610

Prior to transfer, Si, Si/SiO_2, and C-plane sapphire wafers have been cleaned using Nano-Strip (VWR). The silicon substrates have subsequently been immersed in a BOE 10:1 solution to remove the surface oxide formed during the Nano-Strip cleaning step. HOPG and h-BN flakes (2D semiconductors, USA) were mechanically exfoliated and deposited onto sapphire using PDMS (Gel-Pak, USA) prior to transferring CVD graphene on top. The ~15 × 15 mm graphene-templated substrates were inserted into a custom-made physical vapor deposition system, outlined in our previous work.[33] The PVD setup mainly consists of a vertically standing cuvette holding the ZnPc solid source (97%, Sigma-Aldrich) at the bottom and a few-centimeter-long hollow quartz spacer which separates the source from the sample. The reactor pressure was stabilized at ~27 mbar under Ar, while both the source and substrate temperatures were set using independent heater tapes/ropes and PID controllers. The ZnPc source temperature was chosen to be in the 400−450 °C range, in order to have an effective vapor pressure while maintaining a good control over the deposition rate. The substrate temperature was held at 250 °C to favor the β-ZnPc phase, while the reactor pressure was brought to approximately 1.3×10^{-2} mbar during the deposition process.

After ZnPc deposition, the samples were characterized using Raman spectroscopy, field emission scanning electron microscopy (SEM), X-ray diffraction (XRD), and atomic force microscopy (AFM). Graphene and ZnPc were observed using SEM (Zeiss Gemini) with an in-lens detector, a working distance ≤4 mm, and an acceleration voltage ≤3 kV. Raman spectroscopy was carried out using a Witec Apyron system with a 600 gr/mm grating, a 532 nm excitation laser with a power ≤4 mW, and a ×100 lens (Na = 0.9). AFM topography has been acquired using a Bruker Icon system with the quantitative nanomechanical mapping mode (PeakForce) at room temperature with a PeakForce set point in the 4−15 nN range and a scan rate ≤1 Hz. XRD measurements were conducted with a Malvern Panalytical Empyrean III XRD using a Cu radiation source (λ = 1.54059 Å). XRD patterns were fitted using the JADE software (Materials Data Inc).

RESULTS AND DISCUSSION

Influence of the Underlying Substrate. Instead of using a coalesced (i.e., continuous) graphene film, isolated millimeter-size graphene domains were produced on Cu and transferred on the different types of substrates. Partial coverage of the substrate with graphene enables the simultaneous deposition of ZnPc on top of both the graphene and the bare substrate. Using large single-crystalline domains also ensures that graphene grain boundaries, which represent one of the major sources of defects in CVD graphene, do not impact the ZnPc growth. To avoid any process variability, since ZnPc physical vapor deposition depends on various process parameters including the chamber global pressure, the temperature of the source (T_{src}) and the substrate (T_{sub}), and the deposition duration (t_{dep}),[33] the exact same PVD process has been carried out for each sample. Such a process, involving a T_{src} = 450 °C, T_{sub} = 250 °C, and a duration of 30 s, leads to a relatively high ZnPc vaporization rate which results in a uniform and continuous ZnPc coating covering a surface area exceeding 1 cm^2 on each sample.

Figure 1 shows SEM images of ZnPc grown on various graphene-coated substrates including Cu, Si, SiO_2/Si, and C-plane sapphire. The SEM images have been acquired in the vicinity of the graphene domain edges to visualize the ZnPc film deposited on both the graphene-coated (on the left) and the bare substrate (on the right) surfaces. Both plan-view and side-view images show that ZnPc crystallites tend to grow almost vertically when deposited on graphene, while they rather grow horizontally, nearly parallel to the substrate surface when deposited on the bare substrates. SEM images of graphene present on the various substrates before ZnPc deposition can be found in Supporting Information S1.

In the past, differences in MPc crystallite morphology have been attributed to the subtle changes in orientation of the planar organic molecules relative to the underlying substrate. Such an orientation was found to strongly depend on the interplay between the molecule−substrate and molecule−molecule interactions.[26] When the interactions between neighboring molecules prevail over their interaction with the substrate, the molecules tend to adopt an "edge-on" (or "corner-on") orientation. In contrast, when the coupling between MPc molecules and the substrate is strong, the molecules tend to exhibit a "face-on" (or "face-down") orientation. Because the z-axis (corresponding to the normal of the planar ZnPc molecules) differs from the b-axis (corresponding to the molecular stacking direction) depending on the crystal phase (α or β), packing structure (Herringbone or Brickstone), and growth temperature, ZnPc molecules with a face-on orientation form vertical crystallites, while horizontal growth most likely results from an edge-on molecular orientation.[34,35]

The ZnPc horizontal growth direction observed in Figure 1 on bare SiO_2 and sapphire is well-supported by these considerations as organic planar molecules generally weakly interact with insulating materials.[6,36] The similar horizontal growth direction observed on Cu is rather unexpected given that MPc's usually have a strong coupling with metals and should favor a face-on geometry.[6] The experimental observations could, however, simply be explained by the presence of a thin native oxide layer which drastically reduces the ZnPc-Cu coupling. Bare silicon seems to also weakly interact with ZnPc similar to SiO_2 and sapphire. Although particular care has been taken to strip the native oxide and minimize the exposure to air, it remains a challenge to avoid any superficial oxidation when heating samples in a non-UHV PVD system, especially when Si is not protected by graphene.

Although ZnPc morphology seems to be fairly similar regardless of which bare surface it grows on, clear morphological variations are observed when using single-layer graphene as the growth platform. Figure 1a shows that ZnPc crystallites deposited on graphene as-grown on Cu exhibit a nanowire (NW) structure with a height-to-diameter aspect ratio exceeding 40. These NWs are in stark contrast with the continuous thin film obtained when graphene is supported by other substrates (see Figure 1b−d). Depending on the underlying substrate, the sub-micrometer-size ZnPc crystallites rearrange together differently, thus resulting in a different microstructure and surface roughness. The vertical NWs and columnar crystallites are believed to originate from face-on stacking of ZnPc molecules. Although MPc molecules are generally weakly interacting with graphene due to its ultrasmooth dangling bond-free nonpolar structure, the planar molecules were, however, found to adopt the face-on configuration, similarly to the geometry they adopt with strongly interacting metals.[24] Such face-on stacking, allowing the structure stabilization through $\pi-\pi$ interactions, is known

https://doi.org/10.1021/acsomega.1c02758
ACS Omega 2021, 6, 20598−20610

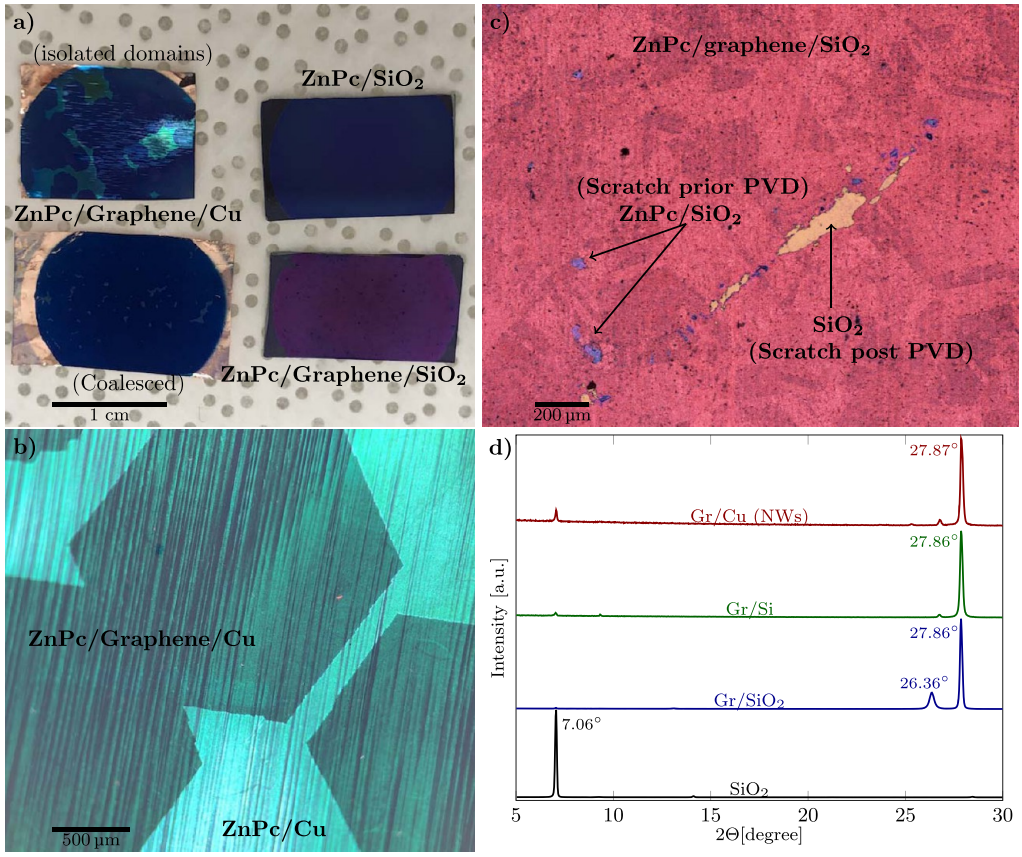

Figure 2. ZnPc deposited on various substrates using a source temperature of 450 °C and a substrate temperature of 250 °C. (a) Photograph of the samples after the PVD of ZnPc. (b) Optical image of ZnPc deposited on isolated hexagonal millimeter-size graphene domains as-grown on Cu foils. (c) Optical image of ZnPc deposited on a continuous graphene film transferred onto SiO_2. (d) XRD spectra of ZnPc deposited on various substrates: bare SiO_2, graphene as-grown on Cu foil, and graphene transferred on Si and SiO_2.

to offer an efficient charge transport perpendicular to the graphene plane, desirable for OPV applications.

Since the graphene present on each substrate is derived from the same CVD growth batch and transferred using the exact same method, it is believed that the observed variations of ZnPc film morphologies originate from the underlying substrate and not directly from the graphene itself. Because graphene is a one-atom-thick layer, its physicochemical properties are more prone to change with the surrounding medium. Therefore, the substrate is expected to exert a significant impact on the ZnPc molecules physisorbed on graphene's top surface.

Molecular Orientation. Figure 1 demonstrates that the presence of graphene or a change in the substrate supporting graphene has a significant impact on ZnPc film coverage and morphology. The ZnPc crystallite growth direction with respect to the substrate surface suggests that the growth template influences the crystal orientation as well. In order to verify the structure of ZnPc molecules deposited on various substrates, X-ray diffraction (XRD) measurements were carried out. In contrast to the first set of ZnPc samples which are based on isolated millimeter-size graphene domains (shown in Figure 1 and in Figure 2a,b), ZnPc was deposited on continuous graphene films (shown in Figure 2a,c) to properly compare the XRD scans. Figure 2d shows that for ZnPc deposited on the bare SiO_2/Si substrate, the most prominent feature is the Bragg reflection observed at $2\Theta = 7.06°$ which corresponds to an interplanar spacing of 12.52 Å. This spacing corresponds to the edge-on MPc orientation and confirms previous assumptions which were based on the literature and SEM images.[34] The peak at $2\Theta = 7.06°$ and the low-intensity peak at $2\Theta = 9.32°$ (d = 9.48 Å) correspond to the (−1 0 1) and (1 0 1) planes which have been attributed to the ZnPc β-phase.[37]

Regardless of the substrate supporting graphene, the most noticeable XRD feature for ZnPc deposited on top of graphene is located at around $2\Theta = 27.86°$. This peak corresponds to an interplanar spacing of 3.20 Å which is characteristic of MPc's lying face-on on the substrate.[24,38,39] The peak at $2\Theta = 26.36°$ is the characteristic (002) peak arising from multilayer graphene.[38] The relatively weak peak at around $2\Theta = 7.06°$ present in the XRD patterns is either due to the fact that graphene is not fully coalesced or because a small amount of graphene has been detached/washed away during the transfer process, thus leaving the bare surface exposed to the ZnPc flux and producing ZnPc with an edge-on geometry. The similar XRD data obtained for the different ZnPc films deposited on graphene suggests that ZnPc planar molecules maintain their face-on orientation, regardless of whether they form nanowires or a thin film structure. The exact correlation between the interplanar distance and the ZnPc packing structure/phase/polymorph is, however, still subject to a great deal of discussion and debate.[3,34,35] It is nevertheless broadly believed that, for most phthalocyanines, the α-phase is metastable and molecules prefer to adopt the more stable β-phase when deposited at $T \geq 210$ °C.[40]

https://doi.org/10.1021/acsomega.1c02758
ACS Omega 2021, 6, 20598−20610

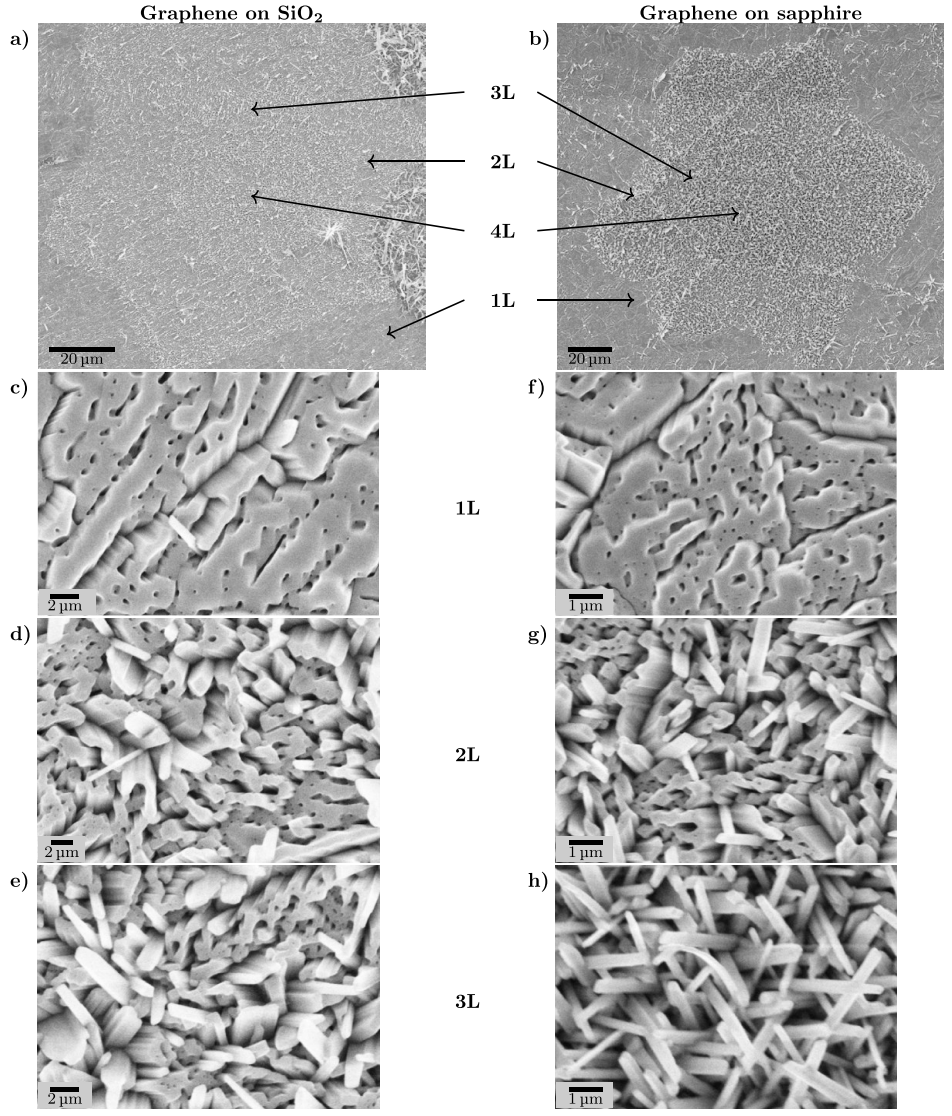

Figure 3. (a,b) Large-area SEM images showing an entire multilayer graphene domain transferred onto (a) SiO_2 and (b) C-plane sapphire after the deposition of ZnPc using a source temperature of 400 °C, a substrate temperature of 250 °C, and a deposition duration of 30 s. (c–e) Higher-magnification SEM images of ZnPc deposited on SiO_2-supported graphene. (f–h) Higher-magnification SEM images of ZnPc deposited on sapphire-supported graphene.

Influence of the Graphene Thickness. To better understand the role of the underlying substrate, ZnPc has also been deposited on top of bi-, tri-, and few-layer graphene. These additional layers increase the separation distance between graphene's top surface and the underlying substrate, thus further screening its potential electrostatic field. These additional graphene layers have been formed at high temperature (1050 °C) during the CVD process by suspending the Cu foils in the CVD reactor. The ad-layers, which originate from the diffusion of C species through the Cu foil, grow underneath the first millimeter-size graphene layer and form the so-called "inverted wedding cake" structure.[31,41] The second and third layers produced for this study typically reach a lateral size of up to 150 and 60 μm, respectively. Using multilayer graphene grown in situ during the CVD process ensures that the interface between graphene layers is smooth and clean, in contrast to multilayer systems obtained by successive manual transfers of single-layer graphene.[42,43] Moreover, highly crystalline domains exhibit primarily zig-zag edges which provide some insights into the relative in-plane orientation of the graphene lattice of each layer.

Figure 3 shows ZnPc grown on single- and multilayer graphene (referred to as 1L, 2L, 3L, and 4L) using the exact same PVD conditions as the ZnPc results presented in Figure 1. ZnPc deposited on graphene-coated SiO_2 and sapphire exhibits a structure progressively transitioning from thin film to nanowires as the graphene thickness increases from 1L to 4L. The formation of high-aspect-ratio nanowires seems to be facilitated on 3L and 4L graphene when supported by sapphire compared to SiO_2. Unfortunately, when depositing ZnPc on graphene as-grown on Cu, the thick, dense, and uniform ZnPc NW coating makes it difficult to perceive any change in morphology with the number of layers, especially using top-view SEM.

While the first set of experiments (presented in Figure 1) suggested that NWs could only be obtained using graphene as-grown on Cu, the second set of experiments shows that transferred graphene can also promote the formation of NWs provided that graphene is sufficiently thick. A major difference

https://doi.org/10.1021/acsomega.1c02758
ACS Omega 2021, 6, 20598−20610

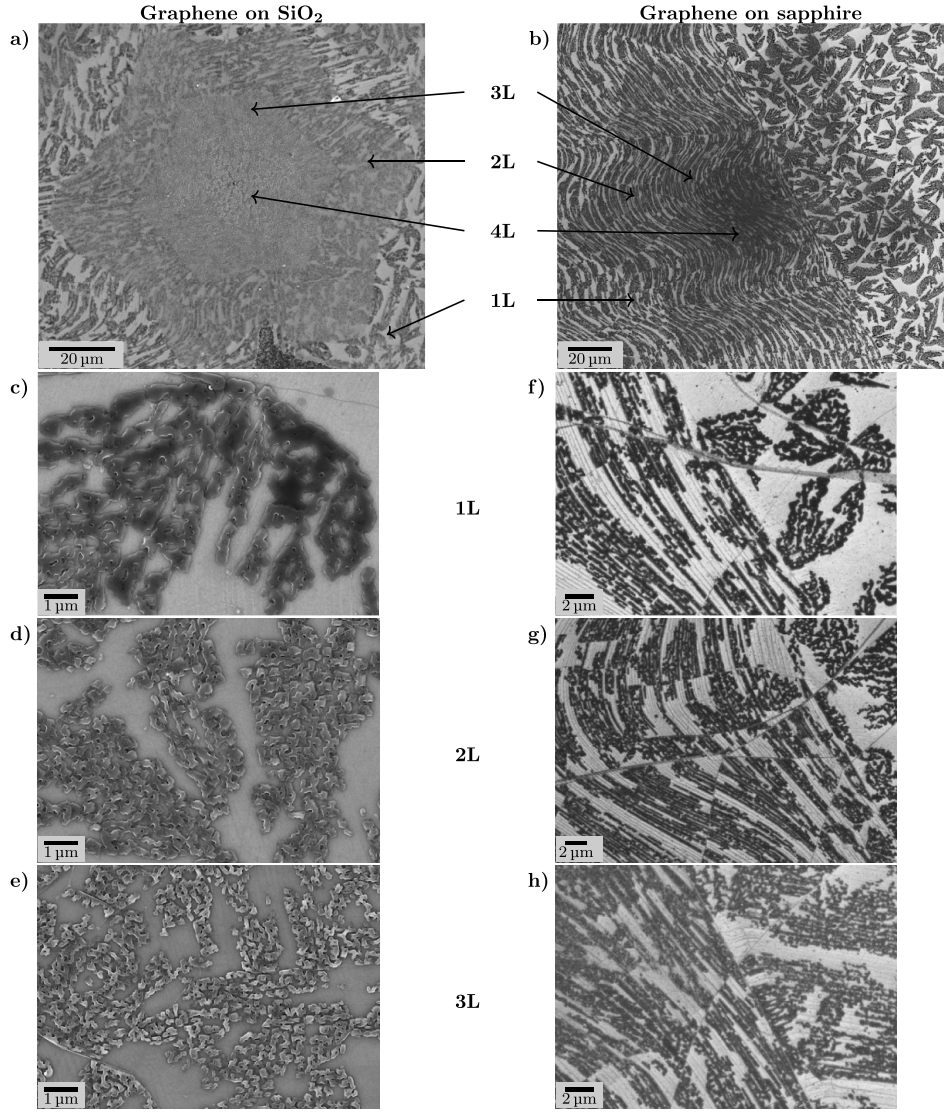

Figure 4. (a,b) Large-area SEM images showing an entire multilayer graphene domain transferred onto (a) SiO_2 and (b) C-plane sapphire after the deposition of ZnPc using a source temperature of 400 °C, a substrate temperature of 250 °C, and a deposition duration of 30 s. (c–e) Higher-magnification SEM images of ZnPc deposited on SiO_2-supported graphene. (f–h) Higher-magnification SEM images of ZnPc deposited on sapphire-supported graphene.

between the as-grown and transferred graphene lies in the fact that the as-grown graphene is much cleaner since the transfer process inevitably leaves the polymer and Cu etching residues on the top and bottom of the graphene layer, respectively. The experimental observations suggest that the potential presence of polymer residues does not represent a major contributor preventing the formation of NWs since they were formed on thicker transferred graphene.

On the other hand, the as-grown graphene is more likely to be in closer contact with the underlying substrate (i.e., the Cu catalyst) than transferred graphene which cannot always perfectly conform to the surface morphology of the substrate. Water molecules and ions are also prone to intercalate between graphene and the substrate, thus reducing the remote effect of the substrate on ZnPc molecules. In this regard, experimental data suggest that the lack of cleanliness underneath graphene could impede the formation of NWs and only a sufficient graphene thickness can efficiently screen the residues' effects to restore the NW growth.

To better understand the interplay between the ZnPc morphology, the underlying substrate, and the number of graphene layers, non-coalesced ZnPc films have also been deposited on top of the various graphene templates. Reducing the deposition flux by decreasing the ZnPc source temperature appears to be a rational approach to decrease the ZnPc amount present on graphene. Indeed, reducing the deposition duration much below 30 s would have a negative impact on the reproducibility and reliability of the PVD process and increasing the pressure would modify the desorption rate of ZnPc molecules physisorbed on the substrate. Moreover, given that the kinetics for the adsorption, surface diffusion, nucleation, and growth are dictated by the substrate temperature, it is essential to keep this parameter constant. According to the ZnPc Antoine equation, reducing T_{src} from 450 to 400 °C decreases the equilibrium vapor pressure from 9.45×10^{-3} mbar to 7.83×10^{-4} mbar.[44] Figure 4 presents the resulting ZnPc film deposited on single- and multilayer graphene predeposited on SiO_2 and C-plane sapphire.

https://doi.org/10.1021/acsomega.1c02758
ACS Omega 2021, 6, 20598−20610

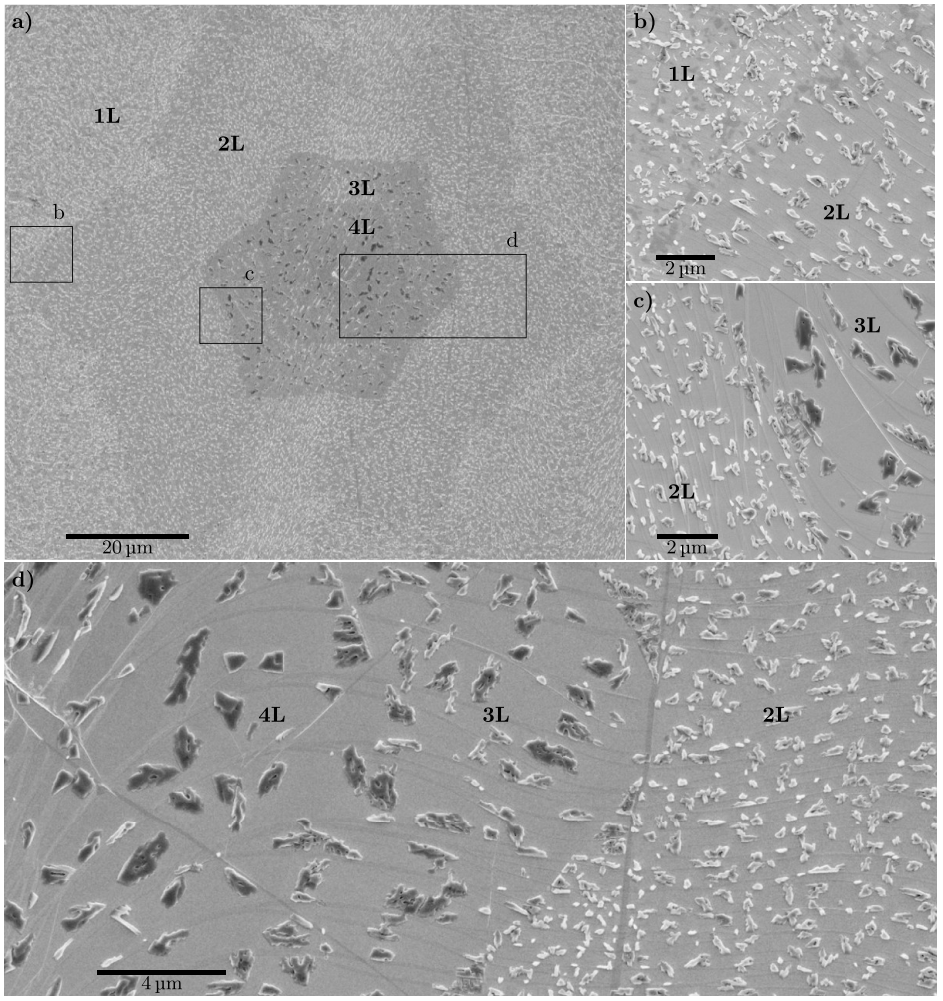

Figure 5. (a) Large-area SEM images showing a multilayer graphene domain as-grown on Cu foil after the deposition of ZnPc using a source temperature of 400 °C, a substrate temperature of 250 °C, and a deposition duration of 30 s. (b–d) SEM images showing the transition (b) from 1L to 2L, (c) from 2L to 3L, and (d) from 2L to 4L.

The early stage of ZnPc film growth consists of the simultaneous presence of isolated ZnPc islands/clusters and bare graphene surface, regardless of the number of graphene layers. This structure suggests that the ZnPc deposited by PVD follows the Volmer–Weber (VW) growth mode rather than the layer-by-layer (i.e., Frank–van der Merwe) or the Stranski–Krastanov (SK) modes. Although VW-like growth modes typically suggest that the intermolecular interaction is stronger than the molecule–graphene interaction, Figures 1 and 3, however, show that ZnPc deposited on transferred graphene tends to cover the entire graphene surface before the film thickening and surface coarsening, thus indicating a non-negligible ZnPc–graphene interaction.

For both SiO_2 and C-plane sapphire substrates, SEM images show that ZnPc crystallites maintain their columnar morphology and vertical orientation regardless of the number of graphene layers underneath. When graphene is supported by SiO_2, the arrangement of the ZnPc crystallites varies with the number of layers. ZnPc crystallites on 1L graphene tend to gather to form individual islands that are barely connected with each other, while ZnPc deposited on 3L rather tends to form an interconnected network made of smaller crystallites. The clustering of crystallites is most likely driven by the minimization of the excess surface energy (associated with the crystallites lateral faces) and facilitated by the high mobility of ZnPc molecules on the graphene surface. In the case of sapphire-supported graphene, the island morphology on 1L, 2L, and 3L looks very similar which is rather intriguing given that ZnPc film morphology obtained under a higher flux strongly varies with the number of layers. Finally, it is worth noting that the ZnPc morphology also slightly depends on whether the various graphene layers are AB-stacked or twisted (as discussed in Supporting Information S2).

Figure 4 also shows the impact of the graphene planar aspect on the growth of ZnPc and more particularly the presence of wrinkles and ripples. The ripples stem from the step-bunching of the Cu surface underneath graphene during the high-temperature CVD process, while wrinkles are mostly due to thermal stress induced by the difference in the expansion coefficient of graphene and its synthesis substrate.[32,45] Graphene ripples, which are easily observable in Figure 4f–h, seem to influence the ZnPc clustering and the shape of the ZnPc islands. Planar graphene with less-pronounced ripples (see bottom right corner of Figure 4a or right half of Figure 4b) is decorated with flower-shaped ZnPc islands. This shape differs from the elongated ZnPc islands deposited on corrugated/rippled graphene. The shape dependency on the planarity of graphene can be explained by the surface diffusion

https://doi.org/10.1021/acsomega.1c02758
ACS Omega 2021, 6, 20598–20610

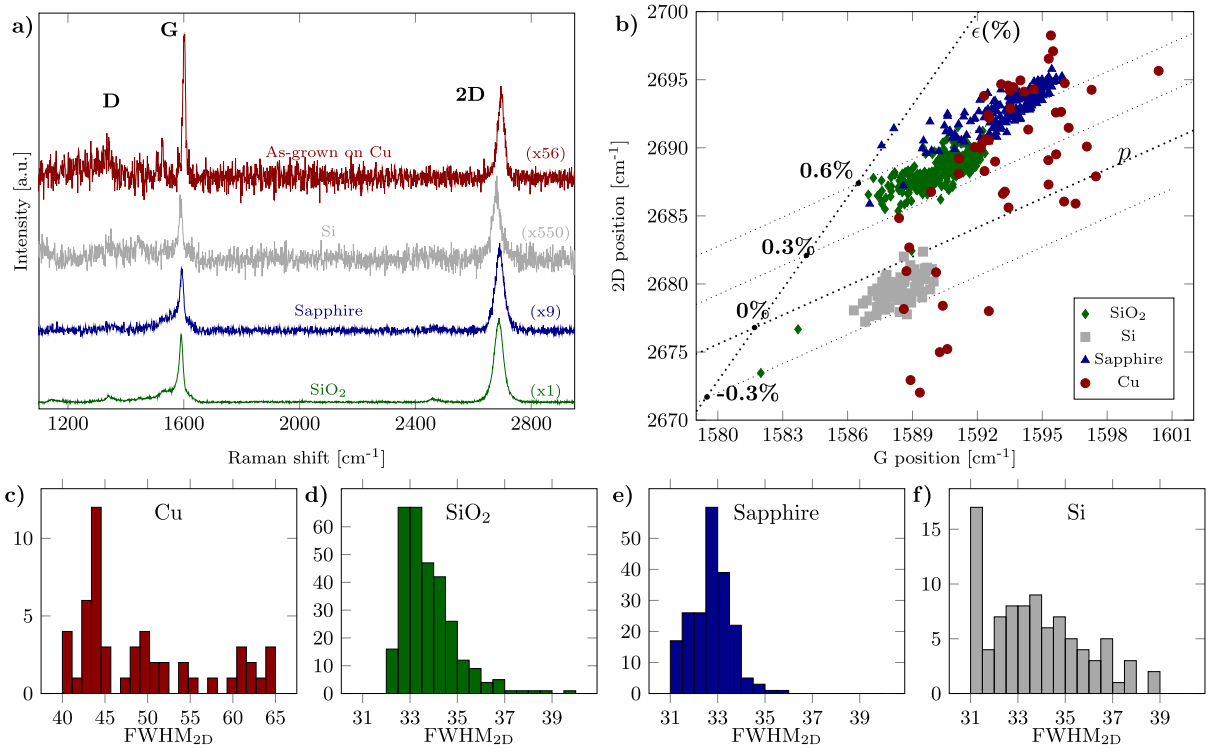

Figure 6. Raman spectroscopy performed on single-layer graphene after 40 min-long annealing at 250 °C. (a) Representative spectra of graphene acquired on various substrates and (b) 2D band position vs G band position for various Raman maps acquired on single-layer graphene on various substrates after annealing. (c–f) Histogram of the 2D band full width at half-maximum for graphene (c) as-grown on Cu and transferred on (d) oxidized silicon, (e) C-plane sapphire, and (f) silicon after annealing. Data in (b–f) are based on Lorentzian fitting of the G and 2D bands.

of ZnPc molecules which is hindered perpendicularly to the ripples and eventually lead to an anisotropic enlargement of the ZnPc islands. Graphene wrinkles seem to also limit the surface diffusion of ZnPc across them. The absence or presence of ripples and wrinkles in graphene eventually dictates the size of the ZnPc grains and most likely impacts the in-plane charge carrier transport within the ZnPc film. Such a phenomenon is discussed in more details in Supporting Information S3. It is, however, worth noting that neither wrinkles nor ripples act as preferential sites for the nucleations of ZnPc islands, which is in stark contrast with the step edges on HOPG as previously reported.[26]

Figure 5 shows the ZnPc growth resulting from the same PVD process as presented in Figure 4 but using single- and multilayer graphene as-grown on Cu. Especially, on 1L and 2L, the graphene surface is decorated with a high density of individual sub-micrometer-size crystallites which do not seem to cluster into larger islands as it is the case on transferred graphene. This phenomenon can be explained by the reduction of the surface diffusion of ZnPc on the as-grown graphene compared to transferred graphene. Given that surface residues generally have an adverse impact on the surface diffusion of adsorbed molecules, this observation provides further evidence that there are little or no residual polymers remaining from the graphene transfer process. The substantial evolution of the ZnPc island size and density with the number of graphene layers as-grown on Cu suggests that the surface diffusion of adsorbed ZnPc molecules improves as the number of graphene layers increases. This finding can result from the Cu terrace enlargement and the decrease in Cu step density when the number of graphene layers increases. The reduction in surface mobility on single-layer graphene can also be explained by an improved interaction induced by the closeness between the ZnPc molecules and the Cu surface. A few studies, however, demonstrated that the issues related to the graphene ripples and wrinkles can easily be addressed by growing graphene on ultraflat Cu(111) templates.[45,46]

The experimental data seem to rule out the potential role of different deposition kinetics. Indeed, by comparing the amount of ZnPc in the SEM images in Figures 4 and 5, it can be noticed that a similar amount of ZnPc has been deposited on graphene regardless of the nature of the underlying substrate. The nanowire formation on the as-grown graphene does not seem to arise from a faster deposition rate.[33]

Although the experimental results clearly show a correlation between ZnPc growth, the type of substrate, and the number of graphene layers, SEM images of ZnPc deposited under two different flux regimes are not sufficient to decipher the fundamental mechanisms responsible for the morphology change. These mechanisms include a change in (i) structural defect in graphene,[47,48] (ii) surface energy,[49] (iii) mechanical strain,[50] and (iv) electrostatic doping[51] or even (v) a change in the substrate-induced polar field through graphene.[30]

In order to identify the major factors responsible for ZnPc morphological change, Raman spectroscopy has been carried out on each graphene substrate (see Figure 6). Prior to Raman characterization, the as-grown and as-transferred graphene samples were annealed for 20 min in the PVD system at 250 °C in order to mimic the state of graphene prior to the ZnPc deposition. Indeed, it is well-documented that thermal energy helps graphene conforming to the underlying substrate,[52] improves the coupling with the underlying substrate,[53] relaxes the short-range growth- and transfer-induced strain,[32,52] and

https://doi.org/10.1021/acsomega.1c02758
ACS Omega 2021, 6, 20598−20610

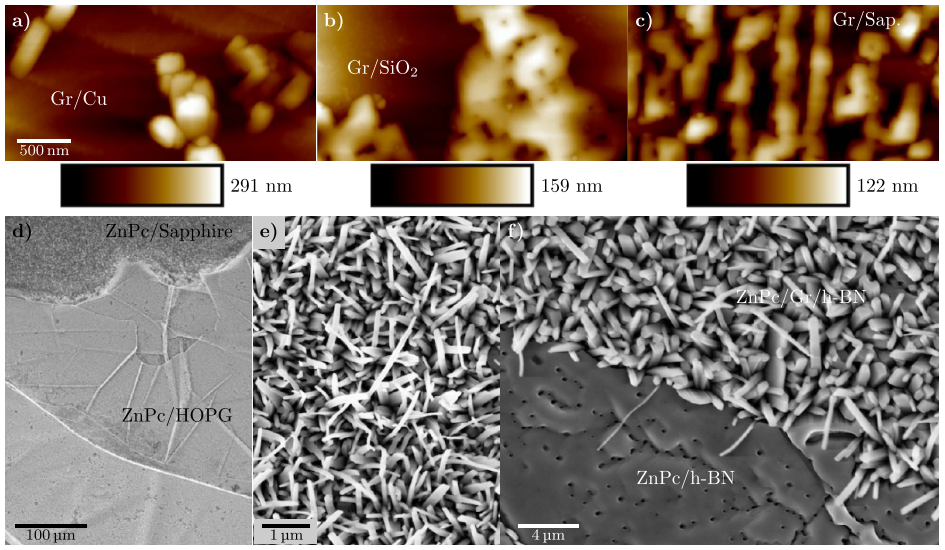

Figure 7. (a–c) AFM images of ZnPc deposited on graphene (a) as-grown on Cu, (b) transferred on SiO_2, and (c) transferred on sapphire, using T_{src} = 400 °C, T_{sub} = 250 °C, and t_{gr} = 30 s. AFM image dimensions: 3 μm × 1.5 μm. (d–f) SEM images of ZnPc deposited using T_{src} = 450 °C, T_{sub} = 250 °C, and t_{gr} = 30 s. (d) ZnPc deposited on a millimeter-size HOPG flake. (e) Higher-magnification image of ZnPc deposited on HOPG. (f) SEM image of ZnPc deposited on single-layer graphene partially covering an exfoliated h-BN flake.

promotes the pyrolysis and desorption of surface impurities/adsorbates.[54]

Figure 6a shows typical Raman spectra of graphene acquired on each substrate. The discrepancy in the signal-to-noise ratio between the various spectra stems from the fact that all spectra were acquired under the same conditions but the spectroscopic response of graphene is drastically influenced by the substrate. The intensity factor used to normalize the 2D band intensity is referred in brackets. The intensity ratio between the D band ($\sim 1350^{-1}$) and the G band ($\sim 1590^{-1}$) is pretty low (≤ 0.1), which attests that a very small amount of structural defects are present in the graphene lattice. This suggests that graphene was not degraded during the transfer procedure and/or during the early stage of the PVD process. Given that graphene deposited on each substrate exhibits similar D-to-G peak intensity ratios, it does not seem like the density of structural defects is responsible for the observed change in ZnPc film morphology and structure.

Various Raman maps have been obtained in different locations of each substrate to obtain statistically robust data about the G band and 2D band ($\sim 2690^{-1}$) positions (ω_G and ω_{2D}, respectively) and full width at half-maximum ($fwhm_{2D}$). The presence of mechanical strain and electrostatic doping in graphene is generally reflected by a shift in the G and 2D peak positions. Strain and doping are decoupled and extracted by plotting ω_G and ω_{2D} (see Figure 6b) similarly to previous works reported in the literature.[52,55]

The clustering of the scatter plots corresponding to graphene transferred on Si (squares), sapphire (triangles), and SiO_2 (diamonds) shows a clear correlation between the type of underlying substrate and the strain present in graphene. Graphene is under a slight tensile strain (~0.15%), a moderate compression strain (~0.45%), and a relatively high compression strain (~0.6%) when it is deposited on Si, SiO_2, or sapphire, respectively.

In contrast to ω_G and ω_{2D} which reflect the average strain within the 1 μm-size Raman spot, the $fwhm_{2D}$ can also be used to compare the presence of strain variation/gradient at the submicrometer scale.[56] Figure 6c–f summarizes the $fwhm_{2D}$ obtained on various substrates for each data point displayed in Figure 6a. Graphene as-grown on Cu exhibits a relatively broad 2D band, averaging at about 49.7 cm^{-1}, which is much wider than for any spectrum acquired on transferred graphene. The sub-micrometer strain gradient present in the as-grown graphene can originate from various factors such as the mismatch strain, the build-in stress accumulated during the CVD cool-down, the graphene sitting on Cu terraces or draping over Cu facets, or even partial Cu oxidation taking place underneath graphene between the CVD and PVD process. These various factors can also explain wide variation of the long-range strain in the as-grown graphene which is reflected by the spreading of the scatter plot (circles) in Figure 6b.

Based on the Raman analysis, it does not seem that the long-range mechanical strain plays a significant role in the ZnPc film morphology given that graphene-coated sapphire and Si substrates host similar ZnPc film morphologies, while graphene experiences opposite strains. The short-range strain variations could, however, be responsible for a change in ZnPc nucleation by changing the adsorption/desorption energy and the surface diffusion, thus explaining the difference in surface diffusion and nucleation observed when comparing ZnPc deposited on graphene on insulators (see Figure 4) and graphene as-grown on Cu (see Figure 5).

The change in ZnPc film morphology can also be caused by a change in adhesion, which is closely related to the surface energy. Due to the extreme thinness of graphene, the surface energy is dictated by the properties of both the surface (i.e., graphene) and the bulk (underlying substrate). According to Fowkes' theory, the surface energy of a solid surface mostly results from multiple forces including dispersive forces and dipole–dipole and ion–dipole interactions.

The polar nature of insulators such as SiO_2 or Al_2O_3 is unlikely to play a significant role in the ZnPc growth through a modification of the electrostatic potential distribution. Indeed, the flat nonpolar ZnPc molecules arriving above graphene would only interact with dipoles generated in the graphene through London forces due to its proximity with the substrate.

https://doi.org/10.1021/acsomega.1c02758
ACS Omega 2021, 6, 20598–20610

This assumption is supported by the fact that ZnPc deposited on graphene-coated Si, SiO_2, or sapphire shows similar growth results, whereas the substrate is either nonpolar covalent-bonded, polar covalent-bonded, or ionic-bonded materials, respectively. Moreover, if the polar component was playing a significant role, ZnPc grown on multilayer graphene supported by polar substrates should be fairly similar to ZnPc grown on single-layer nonpolar materials since the polar field generally decays quickly with the increase in the graphene layers. The experimental observation, however, does not support this presumption.

The Fermi level (i.e., the charge density) of graphene noticeably varies with the underlying substrate as indicated by the Raman analysis in Figure 6b. Graphene as-grown on Cu and transferred on silicon exhibit a relatively high electrostatic doping compared to graphene transferred on insulators, providing evidence of charge transfer with the metallic or semiconducting underlying substrate, respectively. In the case of graphene as-grown on Cu, the wide variation of charge transfer between one Raman acquisition point to another can be attributed to the Cu-graphene closeness (depending on the step-bunching) and to the crystallographic orientation of the Cu grain.[57] The hole doping induced by the underlying SiO_2 and Cu substrates observed here through Raman measurements is consistent with previous experimental and theoretical works.[58,59]

The electrostatic doping or interfacial charge exchange between graphene and the underlying substrate most likely alters the affinity (i.e., strength of the interaction) between graphene and top adsorbates. This phenomenon has been reported by multiple molecular dynamics (MD) simulations studying other systems.[60−64] In the high ZnPc flux deposition regime, the preferential NW growth is observed either on graphene as-grown on Cu or on bare substrates which form quasi-vertical and nearly horizontal high-aspect-ratio crystallites, respectively. In the case of low ZnPc flux deposition regime, the ZnPc crystallites also prefer to adopt NW growth on graphene on Cu, while they prefer to form flat islands on other graphene-coated substrates as evidenced by the AFM images in Figure 7a−c. The AFM height profiles show that the ZnPc islands present on the as-grown graphene are about twice as high as the ZnPc islands deposited on transferred graphene, thus forming early-stage NW stems. This implies that newly adsorbed ZnPc molecules impinging on the as-grown graphene preferentially pile up onto the existing ZnPc island and contribute to vertical growth rather than attaching on graphene and increasing the lateral size of ZnPc islands. The fact that substrates such as Si, SiO_2, and sapphire, through a reduction of the hole-doping (relatively to Cu), strengthen the affinity between ZnPc and graphene and foster the growth of thin ZnPc films, however, does not seem to fully explain all the experimental observations. Indeed, increasing the number of graphene layers (and hence screening/decreasing the doping effect from the substrate) tends to yield similar ZnPc growth results on insulating substrates than on single-layer graphene on the metallic Cu.

In order to shed more light on the underlying mechanisms, ZnPc has been deposited on two additional graphene-based systems: thick (i.e., $\geq$ 20 layers) exfoliated HOPG and CVD graphene transferred on thick exfoliated h-BN. HOPG is broadly viewed as strain-free and electrically neutral, while h-BN offers an ultrasmooth dangling bond-free surface, thus greatly reducing the nanometer-size doping and strain variations in the overlayer graphene lattice.[52,56] Figure 7d−f shows that ZnPc adopts the vertical nanowire morphology on both HOPG and graphene/h-BN, similarly to single- and multilayer graphene on Cu or CVD graphene with more than three layers. These results suggest that, under this PVD regime, the vertical growth into nanowires is the default ZnPc morphology and transferring graphene onto "less ideal" substrates led to a thin film growth unless graphene is thick enough to mitigate the effect of the substrate.

One probable explanation is that transferred graphene is "floating" or "quasi-suspended" on the surface of the target substrate and cannot fully come in close contact with it. ZnPc molecules impinging on the surface thus only interact with suspended graphene and do not experience the electrostatic field of other underlying atoms. In contrast, graphene is in very close contact to the Cu substrate on which it grows and can also conform very well on h-BN which is atomically smooth, thus enabling ZnPc to interact with either Cu or h-BN (remotely through graphene or via dipole formation/hybridization of electronic states in graphene). ZnPc molecules landing on multilayer CVD graphene or HOPG can also interact with a greater number of C atoms compared to a single "suspended" graphene layer due to the closeness of the layers. A stronger electrostatic influence of the underlying substrate (or the graphene underlayers) could make it less preferable for ZnPc to lie on graphene and would drive their vertical stacking. In contrast, suspended single-layer graphene could freely modify its electronic density upon the impingement of ZnPc molecules and provide a better template for the stabilization of ZnPc molecules.

CONCLUSIONS

In summary, we explored the role of the underlying substrate and the number of graphene layers on the ZnPc growth. Highly crystalline single- and multilayer CVD graphene have been produced, transferred, and used as a synthesis template for the physical vapor deposition of ZnPc films with varying crystalline orientations and architectures. Using identical PVD conditions, we demonstrated that ZnPc tends to form high-aspect-ratio nanowires on graphene as-grown on Cu or transferred on h-BN, while it forms a continuous film on graphene transferred on various substrates commonly used in the electronics industry. We also showed that ZnPc film morphology tends to transition from a thin film to a nanowire structure when increasing the thickness of CVD graphene or using HOPG. The observed morphology transitions are discussed based on various physical aspects of graphene (e.g., electrostatic doping, mechanical strain, planarity, structural quality, etc.) which are sensitive to graphene's Supporting Information and modulate the adsorption, surface diffusion, and arrangement of ZnPc molecules. Our results also compare the ZnPc crystalline orientation and film morphology depending on if it is deposited on various substrates and coated or not with a graphene film. Finally, our experiments highlight the role of graphene planarity on the ZnPc film grain size, which is of particular importance for the performance of organic devices wherein charge transport and exciton generation/dissociation are typically limited by grain-size effect and molecular orientation. Our findings demonstrate that the MPc film morphology, structure, and orientation can be controlled by engineering the graphene-based substrate and therefore have significant implications in designing the synthesis template for

https://doi.org/10.1021/acsomega.1c02758
ACS Omega 2021, 6, 20598−20610

the deposition of organic semiconducting functional nanostructures.

■ ASSOCIATED CONTENT

Supporting Information

The Supporting Information is available free of charge at https://pubs.acs.org/doi/10.1021/acsomega.1c02758.

Additional SEM images and texts (PDF)

■ AUTHOR INFORMATION

Corresponding Authors

Benjamin Huet − *Applied Research Laboratory (ARL), The Pennsylvania State University, University Park, Pennsylvania 16802, United States; Department of Materials Science and Engineering and 2D Crystal Consortium (2DCC), Materials Research Institute (MRI), The Pennsylvania State University, University Park, Pennsylvania 16802, United States;* orcid.org/0000-0003-4084-5705; Phone: 814 810 0812; Email: buh462@psu.edu, benjamin.huetb@gmail.com

David W. Snyder − *Applied Research Laboratory (ARL), The Pennsylvania State University, University Park, Pennsylvania 16802, United States*; Email: dws13@arl.psu.edu

Authors

Timothy Mirabito − *Applied Research Laboratory (ARL), The Pennsylvania State University, University Park, Pennsylvania 16802, United States; Department of Materials Science and Engineering and 2D Crystal Consortium (2DCC), Materials Research Institute (MRI), The Pennsylvania State University, University Park, Pennsylvania 16802, United States*

Joan M. Redwing − *Department of Materials Science and Engineering and 2D Crystal Consortium (2DCC), Materials Research Institute (MRI), The Pennsylvania State University, University Park, Pennsylvania 16802, United States;* orcid.org/0000-0002-7906-452X

Complete contact information is available at: https://pubs.acs.org/10.1021/acsomega.1c02758

Notes

The authors declare no competing financial interest.

■ ACKNOWLEDGMENTS

The authors acknowledge the financial support of the National Science Foundation (NSF) through the Penn State 2D Crystal Consortium—Materials Innovation Platform (2DCC-MIP) under NSF cooperative agreement DMR-1539916. T.M. was supported in part by the Penn State Applied Research Laboratory's Exploratory and Foundational Research Program. B.H. was also supported in part by the WBI world excellence fellowships for one year at Penn State University. We gratefully acknowledge the Applied Research Laboratory (ARL), the Nanofabrication Laboratory, and the Materials Characterization Lab (MCL) platforms of Penn State University for the CVD, PVD, and characterization equipment.

■ REFERENCES

(1) Tang, C. W. Two-layer organic photovoltaic cell. *Appl. Phys. Lett.* **1986**, *48*, 183−185.

(2) Peumans, P.; Yakimov, A.; Forrest, S. R. Small molecular weight organic thin-film photodetectors and solar cells. *J. Appl. Phys.* **2003**, *93*, 3693−3723.

(3) Rand, B. P.; Cheyns, D.; Vasseur, K.; Giebink, N. C.; Mothy, S.; Yi, Y.; Coropceanu, V.; Beljonne, D.; Cornil, J.; Brédas, J.-L.; Genoe, J. The Impact of Molecular Orientation on the Photovoltaic Properties of a Phthalocyanine/Fullerene Heterojunction. *Adv. Funct. Mater.* **2012**, *22*, 2987−2995.

(4) Nyokong, T. Effects of substituents on the photochemical and photophysical properties of main group metal phthalocyanines. *Coord. Chem. Rev.* **2007**, *251*, 1707−1722.

(5) Amin, B.; Nazir, S.; Schwingenschlögl, U. Molecular distortion and charge transfer effects in ZnPc/Cu(111). *Sci. Rep.* **2013**, *3*, 1705.

(6) Witte, G.; Wöll, C. Growth of aromatic molecules on solid substrates for applications in organic electronics. *J. Mater. Res.* **2004**, *19*, 1889−1916.

(7) Scarfato, A.; Chang, S.-H.; Kuck, S.; Brede, J.; Hoffmann, G.; Wiesendanger, R. Scanning tunneling microscope study of iron(II) phthalocyanine growth on metals and insulating surfaces. *Surf. Sci.* **2008**, *602*, 677−683.

(8) Karacuban, H.; Lange, M.; Schaffert, J.; Weingart, O.; Wagner, T.; Möller, R. Substrate-induced symmetry reduction of CuPc on Cu(111): An LT-STM study. *Surf. Sci.* **2009**, *603*, L39−L43.

(9) Amin, B.; Nazir, S.; Schwingenschlogl, U. Molecular distortion and charge transfer effects in ZnPc/Cu(111). *Sci. Rep.* **2013**, *3*, 1705.

(10) Cheng, Z. H.; Gao, L.; Deng, Z. T.; Jiang, N.; Liu, Q.; Shi, D. X.; Du, S. X.; Guo, H. M.; Gao, H.-J. Adsorption Behavior of Iron Phthalocyanine on Au(111) Surface at Submonolayer Coverage. *J. Phys. Chem. C* **2007**, *111*, 9240−9244.

(11) Lu, X.; Hipps, K. W. Scanning Tunneling Microscopy of Metal Phthalocyanines: d6and d8Cases. *J. Phys. Chem. B* **1997**, *101*, 5391−5396.

(12) Wang, Y.; Kröger, J.; Berndt, R.; Hofer, W. Structural and Electronic Properties of Ultrathin Tin-Phthalocyanine Films on Ag(111) at the Single-Molecule Level. *Angew. Chem., Int. Ed.* **2009**, *48*, 1261−1265.

(13) Bai, Y.; Buchner, F.; Wendahl, M. T.; Kellner, I.; Bayer, A.; Steinrück, H.-P.; Marbach, H.; Gottfried, J. M. Direct Metalation of a Phthalocyanine Monolayer on Ag(111) with Coadsorbed Iron Atoms. *J. Phys. Chem. C* **2008**, *112*, 6087−6092.

(14) Kim, H.; Bae, S.-H.; Han, T.-H.; Lim, K.-G.; Ahn, J.-H.; Lee, T.-W. Organic solar cells using CVD-grown graphene electrodes. *Nanotechnology* **2013**, *25*, 014012.

(15) Song, Y.; Chang, S.; Gradecak, S.; Kong, J. Visibly-Transparent Organic Solar Cells on Flexible Substrates with All-Graphene Electrodes. *Adv. Energy Mater.* **2016**, *6*, 1600847.

(16) Li, G.; André, N.; Huet, B.; Delhaye, T.; Reckinger, N.; Francis, L. A.; Liao, L.; Raskin, J.-P.; Zeng, Y.; Flandre, D. Enhanced ultraviolet photoresponse in a graphene-gated ultra-thin Si-based photodiode. *J. Phys. D: Appl. Phys.* **2019**, *52*, 245101.

(17) Ren, J.; Meng, S.; Wang, Y.-L.; Ma, X.-C.; Xue, Q.-K.; Kaxiras, E. Properties of copper (fluoro-)phthalocyanine layers deposited on epitaxial graphene. *J. Chem. Phys.* **2011**, *134*, 194706.

(18) McAfee, T.; Gann, E.; Guan, T.; Stuart, S. C.; Rowe, J.; Dougherty, D. B.; Ade, H. Toward Single-Crystal Hybrid-Carbon Electronics: Impact of Graphene Substrate Defect Density on Copper Phthalocyanine Film Growth. *Cryst. Growth Des.* **2014**, *14*, 4394−4401.

(19) Li, G.; Huang, L.; Xu, W.; Que, Y.; Zhang, Y.; Lu, J.; Du, S.; Liu, Y.; Gao, H.-J. Constructing molecular structures on periodic superstructure of graphene/Ru(0001). *Philos. Trans. R. Soc., A* **2014**, *372*, 20130015.

(20) Dou, W.; Huang, S.; Zhang, R. Q.; Lee, C. S. Molecule-substrate interaction channels of metal-phthalocyanines on graphene on Ni(111) surface. *J. Chem. Phys.* **2011**, *134*, 094705.

(21) Uihlein, J.; Polek, M.; Glaser, M.; Adler, H.; Ovsyannikov, R.; Bauer, M.; Ivanovic, M.; Preobrajenski, A. B.; Generalov, A. V.; Chassé, T.; Peisert, H. Influence of Graphene on Charge Transfer between CoPc and Metals: The Role of Graphene-Substrate Coupling. *J. Phys. Chem. C* **2015**, *119*, 15240−15247.

(22) Yang, K.; Xiao, W. D.; Jiang, Y. H.; Zhang, H. G.; Liu, L. W.; Mao, J. H.; Zhou, H. T.; Du, S. X.; Gao, H.-J. Molecule-Substrate

Coupling between Metal Phthalocyanines and Epitaxial Graphene Grown on Ru(0001) and Pt(111). *J. Phys. Chem. C* **2012**, *116*, 14052−14056.
(23) Ying Mao, H.; Wang, R.; Wang, Y.; Chao Niu, T.; Qiang Zhong, J.; Yang Huang, M.; Chen Qi, D.; Ping Loh, K.; Thye Shen Wee, A.; Chen, W. Chemical vapor deposition graphene as structural template to control interfacial molecular orientation of chloroaluminium phthalocyanine. *Appl. Phys. Lett.* **2011**, *99*, 093301.
(24) Xiao, K.; Deng, W.; Keum, J. K.; Yoon, M.; Vlassiouk, I. V.; Clark, K. W.; Li, A.-P.; Kravchenko, I. I.; Gu, G.; Payzant, E. A.; Sumpter, B. G.; Smith, S. C.; Browning, J. F.; Geohegan, D. B. Surface-Induced Orientation Control of CuPc Molecules for the Epitaxial Growth of Highly Ordered Organic Crystals on Graphene. *J. Am. Chem. Soc.* **2013**, *135*, 3680−3687.
(25) Zhang, Y.; Diao, Y.; Lee, H.; Mirabito, T. J.; Johnson, R. W.; Puodziukynaite, E.; John, J.; Carter, K. R.; Emrick, T.; Mannsfeld, S. C. B.; Briseno, A. L. Intrinsic and Extrinsic Parameters for Controlling the Growth of Organic Single-Crystalline Nanopillars in Photovoltaics. *Nano Lett.* **2014**, *14*, 5547−5554.
(26) Wang, T.; Kafle, T. R.; Kattel, B.; Liu, Q.; Wu, J.; Chan, W.-l. Growing Ultra-flat Organic Films on Graphene with a Face-on Stacking via Moderate Molecule-Substrate Interaction. *Sci. Rep.* **2016**, *6*, 28895.
(27) Gonzalez Arellano, D. L.; Burnett, E. K.; Demirci Uzun, S.; Zakashansky, J. A.; Champagne, V. K.; George, M.; Mannsfeld, S. C. B.; Briseno, A. L. Phase Transition of Graphene-Templated Vertical Zinc Phthalocyanine Nanopillars. *J. Am. Chem. Soc.* **2018**, *140*, 8185−8191.
(28) Arellano, D. L. G.; Kolewe, K. W.; Champagne, V. K., III; Kurtz, I. S.; Burnett, E. K.; Zakashansky, J. A.; Arisoy, F. D.; Briseno, A. L.; Schiffman, J. D. Gecko-Inspired Biocidal Organic Nanocrystals Initiated from a Pencil-Drawn Graphite Template. *Sci. Rep.* **2018**, *8*, 11618.
(29) Kim, Y.; et al. Remote epitaxy through graphene enables two-dimensional material-based layer transfer. *Nature* **2017**, *544*, 340−343.
(30) Kong, W.; et al. Polarity governs atomic interaction through two-dimensional materials. *Nat. Mater.* **2018**, *17*, 999−1004.
(31) Huet, B.; Raskin, J.-P. Role of Cu foil in-situ annealing in controlling the size and thickness of CVD graphene domains. *Carbon* **2018**, *129*, 270−280.
(32) Huet, B.; Raskin, J.-P.; Snyder, D. W.; Redwing, J. M. Fundamental limitations in transferred CVD graphene caused by Cu catalyst surface morphology. *Carbon* **2020**, *163*, 95−104.
(33) Mirabito, T.; Huet, B.; Briseno, A. L.; Snyder, D. W. Physical vapor deposition of zinc phthalocyanine nanostructures on oxidized silicon and graphene substrates. *J. Cryst. Growth* **2020**, *533*, 125484.
(34) Kato, M.; Nakaya, M.; Matoba, Y.; Watanabe, S.; Okamoto, K.; Bucher, J.-P.; Onoe, J. Morphological and optical properties of α- and β-phase zinc (II) phthalocyanine thin films for application to organic photovoltaic cells. *J. Chem. Phys.* **2020**, *153*, 144704.
(35) Yoon, Y.; Kim, S.; Choi, H. C. Selective growth of α-form zinc phthalocyanine nanowire crystals via the flow rate control of physical vapor transport. *NPG Asia Mater.* **2020**, *12*, 16.
(36) Verlaak, S.; Steudel, S.; Heremans, P.; Janssen, D.; Deleuze, M. S. Nucleation of organic semiconductors on inert substrates. *Phys. Rev. B: Condens. Matter Mater. Phys.* **2003**, *68*, 195409.
(37) Guo, T.; Zou, T.; Shi, P.; Song, Y.; Wu, M.; Xiao, F.; Zhang, J.; Wu, W.; Wang, H. A new polymorph of zinc-phthalocyanine and its optical properties. *J. Cryst. Growth* **2020**, *546*, 125760.
(38) Wang, S. D.; Dong, X.; Lee, C. S.; Lee, S. T. Orderly Growth of Copper Phthalocyanine on Highly Oriented Pyrolytic Graphite (HOPG) at High Substrate Temperatures. *J. Phys. Chem. B* **2004**, *108*, 1529−1532.
(39) Dou, W.-D.; Lee, C.-S. Controllable growth of copper-phthalocyanine thin film on rough graphene substrate. *Appl. Phys. Lett.* **2014**, *105*, 223110.
(40) Senthilarasu, S.; Hahn, Y. B.; Lee, S.-H. Structural analysis of zinc phthalocyanine (ZnPc) thin films: X-ray diffraction study. *J. Appl. Phys.* **2007**, *102*, 043512.
(41) Nie, S.; Wu, W.; Xing, S.; Yu, Q.; Bao, J.; Pei, S.-s.; McCarty, K. F. Growth from below: bilayer graphene on copper by chemical vapor deposition. *New J. Phys.* **2012**, *14*, 093028.
(42) Purdie, D. G.; Pugno, N. M.; Taniguchi, T.; Watanabe, K.; Ferrari, A. C.; Lombardo, A. Cleaning interfaces in layered materials heterostructures. *Nat. Commun.* **2018**, *9*, 5387.
(43) Schwartz, J. J.; Chuang, H.-J.; Rosenberger, M. R.; Sivaram, S. V.; McCreary, K. M.; Jonker, B. T.; Centrone, A. Chemical Identification of Interlayer Contaminants within van der Waals Heterostructures. *ACS Appl. Mater. Interfaces* **2019**, *11*, 25578−25585.
(44) Semyannikov, P. P.; Basova, T.V.; Trubin, S. V.; Kol'Tsov, E. K.; Plyashkevich, V. A.; Igumenov, I. K. Vapor pressure of some metal phthalocyanines. *Russ. J. Phys. Chem. A* **2008**, *82*, 159−163.
(45) Huet, B.; Raskin, J.-P. Role of the Cu substrate in the growth of ultra-flat crack-free highly-crystalline single-layer graphene. *Nanoscale* **2018**, *10*, 21898−21909.
(46) Huet, B.; Zhang, X.; Redwing, J. M.; Snyder, D. W.; Raskin, J.-P. Multi-wafer batch synthesis of graphene on Cu films by quasi-static flow chemical vapor deposition. *2D Mater.* **2019**, *6*, 045032.
(47) Dou, W.; Yang, Q.; Lee, C.-S. Influences of Ion-Induced Defects on Growth of Copper-Phthalocyanine Film on Graphene Substrates. *J. Phys. Chem. C* **2012**, *116*, 19278−19284.
(48) Nalamati, S.; Devkota, S.; Li, J.; Lavelle, R.; Huet, B.; Snyder, D.; Penn, A.; Garcia, R.; Reynolds, L.; Iyer, S. Hybrid GaAsSb/GaAs Heterostructure Core-Shell Nanowire/Graphene and Photodetector Applications. *ACS Appl. Electron. Mater.* **2020**, *2*, 3109−3120.
(49) Yuan, X.; Yang, J.; He, J.; Tan, H. H.; Jagadish, C. Role of surface energy in nanowire growth. *J. Phys. D: Appl. Phys.* **2018**, *51*, 283002.
(50) Bissett, M. A.; Konabe, S.; Okada, S.; Tsuji, M.; Ago, H. Enhanced Chemical Reactivity of Graphene Induced by Mechanical Strain. *ACS Nano* **2013**, *7*, 10335−10343.
(51) Huttmann, F.; Martínez-Galera, A. J.; Caciuc, V.; Atodiresei, N.; Schumacher, S.; Standop, S.; Hamada, I.; Wehling, T. O.; Blügel, S.; Michely, T. Tuning the van der Waals Interaction of Graphene with Molecules via Doping. *Phys. Rev. Lett.* **2015**, *115*, 236101.
(52) Lee, J. E.; Ahn, G.; Shim, J.; Lee, Y. S.; Ryu, S. Optical separation of mechanical strain from charge doping in graphene. *Nat. Commun.* **2012**, *3*, 1024.
(53) Cheng, Z.; Zhou, Q.; Wang, C.; Li, Q.; Wang, C.; Fang, Y. Toward Intrinsic Graphene Surfaces: A Systematic Study on Thermal Annealing and Wet-Chemical Treatment of SiO2-Supported Graphene Devices. *Nano Lett.* **2011**, *11*, 767−771.
(54) Pirkle, A.; Chan, J.; Venugopal, A.; Hinojos, D.; Magnuson, C. W.; McDonnell, S.; Colombo, L.; Vogel, E. M.; Ruoff, R. S.; Wallace, R. M. The effect of chemical residues on the physical and electrical properties of chemical vapor deposited graphene transferred to SiO2. *Appl. Phys. Lett.* **2011**, *99*, 122108.
(55) Bendiab, N.; Renard, J.; Schwarz, C.; Reserbat-Plantey, A.; Djevahirdjian, L.; Bouchiat, V.; Coraux, J.; Marty, L. Unravelling external perturbation effects on the optical phonon response of graphene. *J. Raman Spectrosc.* **2018**, *49*, 130−145.
(56) Neumann, C.; Reichardt, S.; Venezuela, P.; Drögeler, M.; Banszerus, L.; Schmitz, M.; Watanabe, K.; Taniguchi, T.; Mauri, F.; Beschoten, B.; Rotkin, S. V.; Stampfer, C. Raman spectroscopy as probe of nanometre-scale strain variations in graphene. *Nat. Commun.* **2015**, *6*, 8429.
(57) Frank, O.; Vejpravova, J.; Holy, V.; Kavan, L.; Kalbac, M. Interaction between graphene and copper substrate: The role of lattice orientation. *Carbon* **2014**, *68*, 440−451.
(58) Giovannetti, G.; Khomyakov, P. A.; Brocks, G.; Karpan, V. M.; van den Brink, J.; Kelly, P. J. Doping Graphene with Metal Contacts. *Phys. Rev. Lett.* **2008**, *101*, 026803.
(59) Ryu, S.; Liu, L.; Berciaud, S.; Yu, Y.-J.; Liu, H.; Kim, P.; Flynn, G. W.; Brus, L. E. Atmospheric Oxygen Binding and Hole Doping in

https://doi.org/10.1021/acsomega.1c02758
ACS Omega 2021, 6, 20598−20610

Deformed Graphene on a SiO2Substrate. *Nano Lett.* **2010**, *10*, 4944−4951.
(60) Ashraf, A.; Wu, Y.; Wang, M. C.; Yong, K.; Sun, T.; Jing, Y.; Haasch, R. T.; Aluru, N. R.; Nam, S. Doping-Induced Tunable Wettability and Adhesion of Graphene. *Nano Lett.* **2016**, *16*, 4708−4712.
(61) Förster, G. D.; Rabilloud, F.; Calvo, F. Adsorption of metal nanoparticles on carbon substrates and epitaxial graphene: Assessing models for dispersion forces. *Phys. Rev. B* **2015**, *91*, 245433.
(62) Lai, C.-Y.; Tang, T.-C.; Amadei, C. A.; Marsden, A. J.; Verdaguer, A.; Wilson, N.; Chiesa, M. A nanoscopic approach to studying evolution in graphene wettability. *Carbon* **2014**, *80*, 784−792.
(63) Guo, Y.; Guo, W. Effects of graphene coating and charge injection on water adsorption of solid surfaces. *Nanoscale* **2013**, *5*, 10414−10419.
(64) Mehdipour, H.; Smith, B. A.; Rezakhani, A. T.; Tafreshi, S. S.; de Leeuw, N. H.; Prezhdo, O. V.; Moshfegh, A. Z.; Akimov, A. V. Dependence of electron transfer dynamics on the number of graphene layers in π-stacked 2D materials: insights from ab initio nonadiabatic molecular dynamics. *Phys. Chem. Chem. Phys.* **2019**, *21*, 23198−23208.

https://doi.org/10.1021/acsomega.1c02758
ACS Omega 2021, 6, 20598−20610